MASTERARBEIT | MASTER'S THESIS

Titel | Title

Evolution of the forefield of the Bachfallenferner, Stubai Alps, Austria: Sedimentological response to rapid change

verfasst von | submitted by

Sara Karbacher BSc

angestrebter akademischer Grad | in partial fulfilment of the requirements for the degree of

Master of Science (MSc)

Wien | Vienna, 2025

Studienkennzahl lt. Studienblatt | Degree programme code as it appears on the student record sheet:	UA 066 815
Studienrichtung lt. Studienblatt | Degree programme as it appears on the student record sheet:	Masterstudium Erdwissenschaften
Betreut von | Supervisor:	Univ.-Prof. Daniel Le Heron PhD

EVOLUTION OF THE FOREFIELD OF THE BACHFALLENFERNER, STUBAI ALPS, AUSTRIA

SEDIMENTOLOGICAL RESPONSE TO RAPID CHANGE

ABSTRACT

This paper describes and interprets the sedimentological and geomorphological evolution of the Bachfallenferner (Stubai Alps, Austria) glacial margin in the context of its retreat since 1997. Using a high-quality set of aerial photographs collected by a MAVIC Mini 4 UAV, this study presents the first known map of the forefield in recent times, revealing a thick till sheet with flutes and initiating boulders, a dynamic delta system, a proglacial lake, and extensive supraglacial debris. These images allow the evolution of the forefield to be documented, allowing the initiation, expansion and development of an ice-contact lake to be understood. Moreover, the time series allows the development of a large debris cone on the ice to be documented, which as of 2024 measures 250 m long, up to 100 m wide and 30 m high. Clast analysis (N=90) indicates that supraglacial debris is dominated by angular mica schist and quartz gneiss, primarily sourced from surrounding valley walls via rockfall.

Field observations and geomorphological mapping indicate that debris cover on the Bachfallenferner has expanded substantially since 1997. This expansion appears to result from a combination of englacial transport and direct sediment input from the surrounding topography. One notable outcome is the formation of a prominent debris cone, for which three possible formation mechanisms have been proposed: (i) control by subglacial morphology, (ii) initiation by a major rockfall event, and (iii) influence of subglacial hydrological processes.

The Bachfallenferner therefore serves as a small-scale analogue for debris-covered glaciers elsewhere in the European Alps, illustrating how rockfall supply, ice dynamics and meltwater feedback interact to reshape supraglacial, subglacial and proglacial systems under rapid climate warming.

KURZFASSUNG

Diese Arbeit beschreibt und interpretiert die sedimentologische sowie geomorphologische Entwicklung des Bachfallenferners (Stubaier Alpen, Österreich) und dessen rasanten Rückzug seit dem Jahr 1997. Anhand hochauflösender Luftbilder, aufgenommen mit dem MAVIC Mini 4 UAV, wurde erstmals eine detaillierte geomorphologische Karte des Gletschervorfeldes erstellt.

Eine Klastenanalyse *(clast analysis)* (N=90) zeigt, dass das supraglaziale Material größtenteils aus Glimmerschiefer und Quarzgneis besteht, dass von den umliegenden Talflanken stammt und durch Steinschlag auf die Gletscheroberfläche gelangt ist. Feldbeobachtungen sowie historisches Bildmaterial lassen erkennen, dass sich die supraglaziale Schuttbedeckung seit 1997 erheblich vergrößert hat. Diese Ausdehnung scheint auf eine Kombination aus englazialem Transport und direktem Eintrag aus der umliegenden Topografie zurückzuführen zu sein.

Zudem wurde die Entstehung und Entwicklung eines Schuttkegels *(debris cone)* auf der Gletscheroberfläche aufgezeigt, der im Jahr 2024, eine Länge von 250 m, eine maximale Breite von 100 m und eine Höhe von bis zu 30 m erreichte. Zur Erklärung der Genese dieses Schuttkegels wurden drei Prozesse angenommen: (i) Beschaffenheit er subglaziale Morphologie, (ii) Auswirkung großer Steinschlagereignisse und (iii) Einfluss subglazialer hydrologischer Prozesse.

Der Bachfallenferner dient daher als kleinräumiges Beispiel für schuttbedeckte Gletscher an vergleichbaren Standorten in den Alpen. Das Untersuchungsgebiet veranschaulicht, wie ein rascher Gletscherrückzug infolge erheblicher Klimaerwärmung in Kombination mit Schuttbedeckung, supraglaziale, subglaziale sowie proglaziale Systeme tiefgreifend verändern kann.

CONTENTS

01 INTRODUCTION

Mountain glaciers are themselves influenced by climate, and they in turn influence the landscape and oceans (Benn and Evans, 2010). Given the rapid climate warming in the European Alps, glacier retreat is one of the most visible impacts in high mountain landscapes. Across the Alps, glaciers have experienced a drastic reduction in size and volume due to rising air temperatures and shifting precipitation patterns, both of which contribute to increased glacier melt. The most significant driver of glacier retreat has been the exceptionally high summer temperatures, particularly in the months of June, July and August. In Austria, during the ablation period of 2024, the average temperature was 1,7°C higher than the reference climate period of 1981-2010. The temperatures for all months in 2023/24, except November 2023 and September 2024, exceeded those of the climate reference period (Lieb and Kellerer-Pirklbauer, 2025). Alongside high summer temperatures, low precipitation levels in July and August, as well as the absence of summer snowfall, has further intensified glacier loss.

In Austria, glaciers have lost more than 50 % of their total area and two-thirds of their volume since the Little Ice Age around 1850 (Fischer et al., 2015; Helfricht et al., 2019). This trend has accelerated in recent years, with Austrian glaciers experiencing a 10% volume loss in just two years. The current largest glacier of Austria (the Pasterze Glacier) in Corinthia retreated 203.5 m in 2022/23 and lost a total ice volume of 14.03 Mio m^3 (Lieb and Kellerer-Pirklbauer, 2024). In Tirol, the Ötztal Alps, have witnessed comparable glacier shrinkage, with projections indicating that up to 80% of their ice mass could disappear by 2100 under a 3°C warming scenario (Hanzer et al., 2018). Within the top ten receding glaciers of Austria, two (Fernauferner and Alpeinerferner) are situated close to the study area in the Stubai Alps (Lieb and Kellerer-Pirklbauer, 2024, 2025).

Glacier length measurements of the Bachfallenferner showed a retreat of 400 m during the time span 2002-2024, and the glacier lost 120 m of its total length in the time span 2019 – 2024 (Lieb and Kellerer-Pirklbauer, 2024, 2025). This retreat led to exposure of geomorphological structures and sedimentary deposits that have never been mapped before. The aim of this thesis is to present detailed mapping and analysis of geomorphological features and sedimentary deposits at the forefield of the Bachfallenferner. By comparing these features with historical data, their formation and impact on the landscape can be understood, and their potential role in a geohazard context can be evaluated.

02 STUDY AREA

The Stubai Alps are part of the Eastern Alps, primarily located in Tyrol, Austria, with portions extending into South Tyrol, Italy. The study site is situated at the northern end of the Sulz Valley, a tributary of the Ötztal Valley. The Bachfallenferner lies between the Putzenkarschneid to the east and the Bachfallenkopf to the west, with the Gaislehnkogel to the south and the Grüne Tatzen to the north. Its meltwater feeds the Winnebach River *(Fig. 1)*. Based on 2023 Google Earth satellite imagery, the Bachfallenferner had an estimated area of 1,25 km^2, with 18.188 m^2 of exposed bedrock in the central-southern part of the glacier. In contrast to the relatively small Bachfallenferner, the Übeltalferner, the largest glacier in the Stubai Alps, covered 5.71 km^2, followed by the Sulzenauferner, which had an area of 3.11 km^2, both based on 2021 Google Earth satellite imagery.

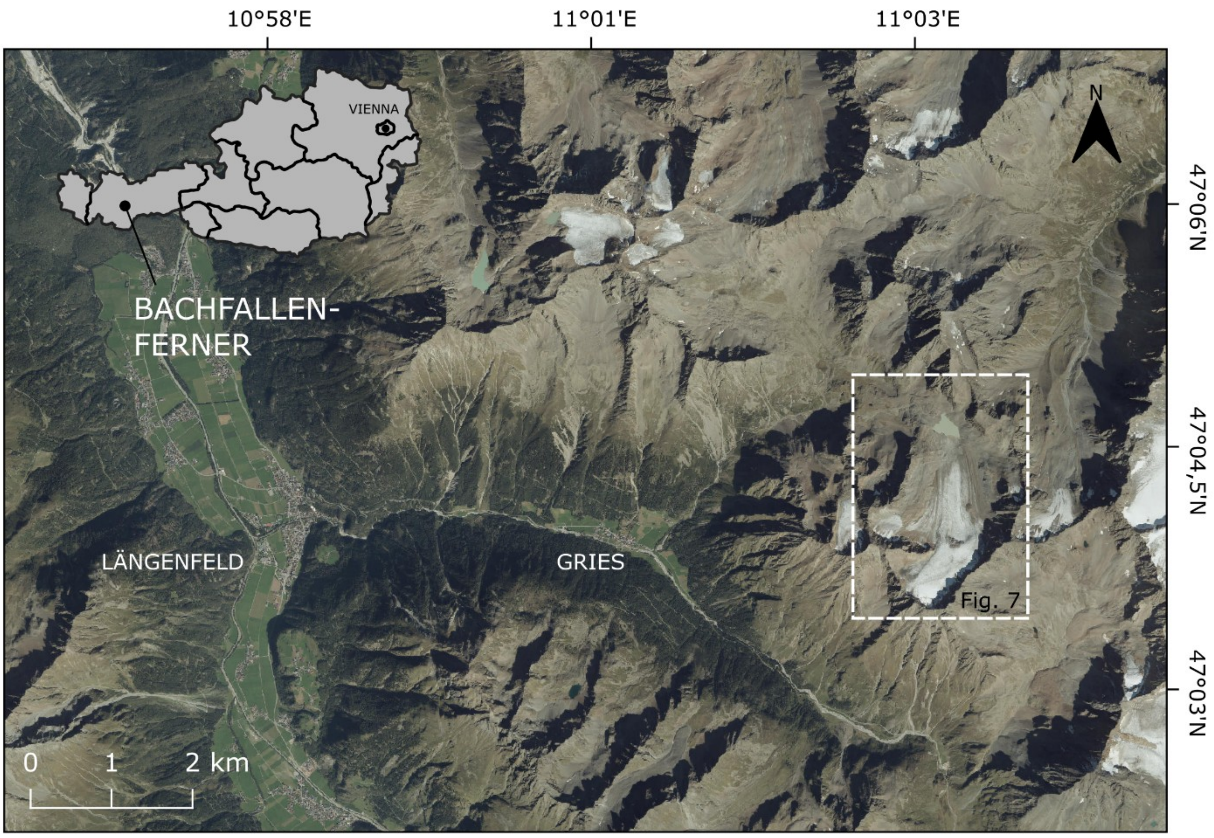

Figure 1: Location map of the study site of the Bachfallenferner in the western Stubai Alps (Stadt Wien und Österreichische Länder bzw. Ämter der Landesregierung, 2021, downloaded April 7, 2025 from maps.wien.gv.at/basemap/1.0.0/WMTSCapabilities.xml)

03 PREVIOUS RESEARCH

Geological mapping of the Ötztal and Stubai Alps was conducted a century ago (Hammer, 1925, 1929). The map of Hammer and Ohnesorge (1929) provides a detailed description of the region's lithologies and remains a reliable reference today. The principal lithologies include biotite-plagioclase gneiss, mica schist and quartzite. All these rock types are present in the surroundings of the Bachfallenferner (Fig. 2). The so-called Winnebach migmatite represents a distinct characteristic of the area and has consequently been the central focus of previous research (Hoinkes, 1973; Hoinkes et al., 1972; Klötzli-Chowanetz et al., 1997) at the study site. The Winnebach migmatite is the product of a high-grade metamorphic event led to a locally in-situ anatexis (partial melting) within the biotite-plagioclase gneiss (Hoinkes et al., 1972, 2021) and subsequently to an intrusion into the granodioritic-tonalitic magma (Schindlmayr, 1999). Single zircon evaporation Pb-Pb analysis and U-Pb zircon dating indicate that the partial anatexis occurred around 490 Ma, which can be attributed to the Early Ordovician orogenic cycle (Klötzli-Chowanetz et al., 1997).

The Bachfallenferner has been monitored since the late 19th century (World Glacier Monitoring Service, 2024). Figure 3 summarizes front variations of the Bachfallenferner from 1891 to 2020, illustrating a steady decline in the glacier's length, with a notably accelerated retreat since 2010. According to the Austrian Glacier Inventory 2 (GI2, Stubai Alps 1997) the average ice thickness is 41 m, with an estimated volume of 0.086 km^3. Ground-penetrating radar (GPR) surveys of the Bachfallenferner were conducted in 2000, followed by inventory comparisons in 2006. During the surveyed period (1997-2006), the glacier experienced a surface elevation decrease of -2.4 m (Fischer and Kuhn, 2013; Lambrecht and Kuhn, 2007). Fischer *et al.* (2015) expanded the Austrian glacier inventory (GI3, Stubai Alps 2006). In 2006, the glaciers in the Stubai Alps covered an area of 49.42 km^2, representing a 23% reduction in glacier coverage between 1997 and 2006. By 2015, the total glacier area in the Stubai Alps has further decreased to 37 km^2 (Buckel et al., 2018). Since then, no further attempts to create an up-to-date glacier inventory in Austria have been made.

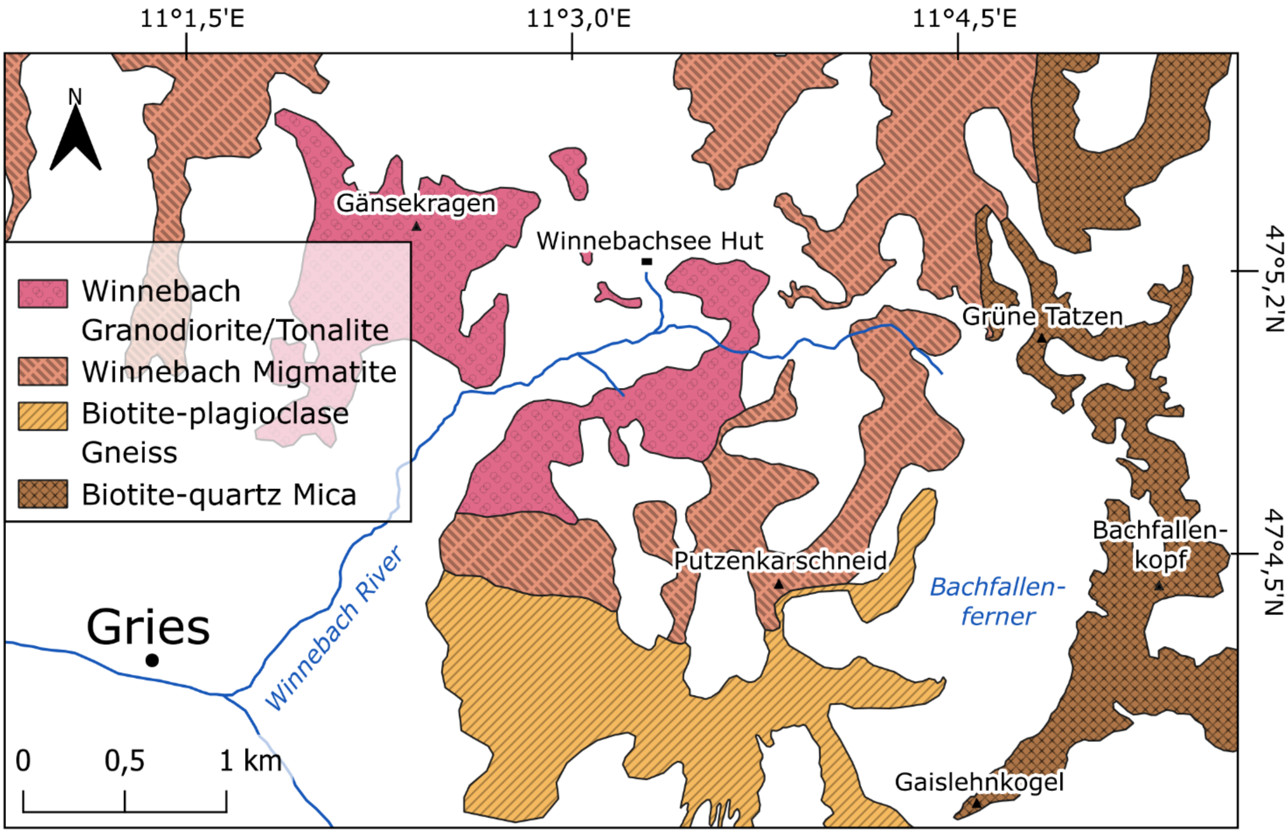

Figure 2: Geological overview map of Bachfallenferner region ((Hoinkes et al., 1972, 2021) mod. version)

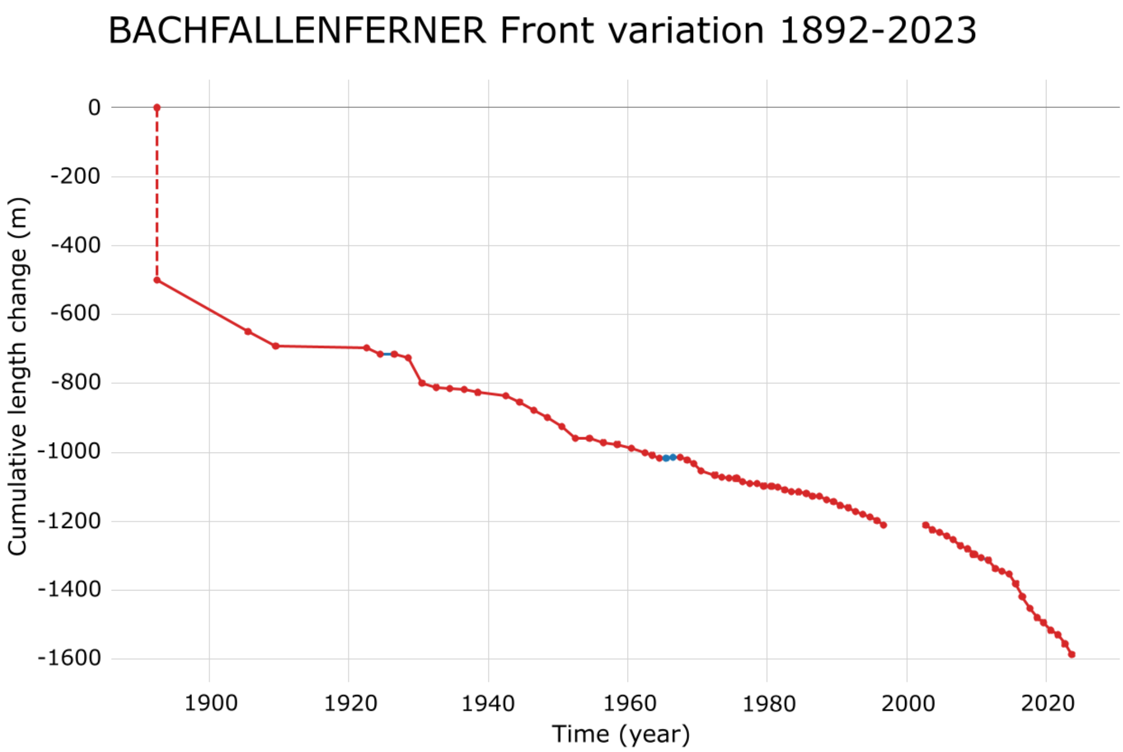

Figure 3: Front variations between 1892-2023 of Bachfallenferner. Red dots indicate glacier retreat, while blue dots represent glacier advance (World Glacier Monitoring Service, 2024)

04 GLACIATIONS

The Quaternary period, spanning the last 2.58 million years, was characterized by four major glaciations that shaped the Europeans Alps. These glaciers are classified into Günz (MIS 16, 676-621 ka), Mindel (MIS 12, 478-424 ka), Riss (MIS 6, 191-130 ka) and Würm (MIS 2, 29-12) (Reitner, 2022). Each of these glacial periods was marked by extensive ice advances, followed by warmer interglacial periods that allowed for the retreat of glaciers. During the Last Glacial Maximum (LGM, 31-21 ka), glaciers in the Eastern Alps advanced significantly, filling major valleys and extending into the foreland (van Husen, 1997). Initially, topographical constraints restricted their growth to tributary valleys despite the cold climate. Rapid ice buildup around 24 ka ago led to the development of ice streams and piedmont glaciers. However, the glaciers began retreating rapidly after the LGM, becoming largely ice-free within a few hundred years. This retreat was interrupted by short-lived glacier oscillations, such as the Gschnitz stadial around 14 ka ago, which left behind well-preserved terminal moraines (van Husen, 1997).

The most recent significant glacial advance occurred during the Little Ice Age (LIA) between the 13th and 19th century, with its peak often placed between 1850 and 1860, marking the maximum glacier extent and the beginning of their retreat (Nicolussi et al., 2022). This period saw widespread glacier expansion across the Alps, leaving behind well-defined terminal moraines, outwash plains and trimlines, which remain clearly visible today. The glacial and periglacial landforms formed during the LIA provide exceptionally well-preserved evidence of past climatic conditions, providing a crucial reference for reconstructing earlier cooling phases, of which the geomorphic and sedimentary evidence are less distinct due to subsequent landscape modifications (Reitner, 2022). Based on these distinct remnants Fischer *et al.* (2015) successfully mapped the extent of the LIA glaciers throughout the Austrian Alps.

05 GLACIAL AND PERIGLACIAL GEOMORPHOLOGY

High alpine areas are significantly influenced by glacial, periglacial and gravitational processes. These geomorphic processes contribute to the shaping of landscapes through erosion, transportation and deposition of sediments, leading to the development of distinct landforms that characterize high mountainous environments.

Glacial processes can be categorized into supraglacial, englacial, proglacial and subglacial processes. Supraglacial processes occur at the surface of glaciers and involve the melting, transport and deposition of debris. One of the most notable features resulting from these processes is the moulin, a vertical shaft that develops within the glacier as meltwater exploits crevasses and subsequently reaches the glacier bed, facilitating basal melting and influencing subglacial hydrology (Benn and Evans, 2010). Additionally, debris cones develop as a result of differential melting on the glacier surface (Østrem, 1959; Swithinbank, 1950). These are characterized by a core of ice enveloped by a layer of supraglacial debris. The debris cover serves as an insulating layer, protecting the underlying ice from ablation. As the surrounding glacier surface undergoes differential melting and lowers, the insulated ice beneath the debris remains intact, leading to the formation of a conical structure. The sides of the cone steepen until they reach an angle where the debris becomes unstable and cascades downward, further protecting the ice core and contributing to the cone's growth. This process continues until a balance is achieved between the insulating effect of the debris and the melting of the ice (Hénot et al., 2023; Swithinbank, 1950). Englacial processes occur within the ice mass and comprise the transport of meltwater and debris through a system of internal conduits. These processes can lead to the formation of cryoconite holes, which develop when dust or organic material accumulate in depression on the ice surface, accelerating localized melting. Subglacial processes play a fundamental role in shaping the basal landscape beneath glaciers, driven by a combination of abrasion, quarrying and sediment deformation. The most prominent feature of glacial erosion are striations, which form when hard rock debris is dragged along the bedrock surface at the base of the glacier. These linear grooves serve as an indicator of glacier flow direction. Further evidence of glacial erosion is provided via features such as roche moutonnées. As a glacier move downvalley, friction between the ice and bedrock causes localized melting at the base. Meltwater seeps into cracks, where is subsequently refreezes, expanding and creating additional fractures in the rock. This repeated freeze-thaw cycle, known as regulation, gradually weakens the bedrock until fragments break free and become entrapped within the glacier (Kumar, 2011). The asymmetrical shape of the roche moutonnée originates from the combination of abrasion and plucking. The upstream side is smooth and polished by the glacier as it moves over the surface, while the downstream side is rough and steep due to glacial plucking.

In addition to erosional structures, depositional subglacial landforms are also produced in the subglacial environment. Among these, flutes are well represented in Alpine terrain and comprise elongated ridges of sediment oriented parallel to the flow direction of the glacier. According to the Cavity Infill Model (Ives and Iverson, 2019), a flute begins to form when basal melting traps a boulder on the subglacial bed. As glacial ice passes by, it is forced to flow around the lodged boulder, creating an elongated cavity in the ice parallel to its flow. The pressure from the overlying glacial ice then fills this cavity with water-soaked till. As the glacier melts and retreats, it reveals the till bed and the resulting long, low ridges of till shaped upon it. Flutes serve as indicators of temperate or warm-based glaciers. Proglacial processes are active in areas beyond the glacier terminus, where meltwater and sediment interact to create diverse depositional features. These processes facilitate the accumulation and redistribution of sediments through glaciofluvial and glaciolacustrine dynamics, shaping the proglacial landscape (Bennett and Glasser, 2009). Moraines develop through accumulation and deposition of glacially transported debris, consisting of loose sediment and rock fragments, known as till, at various points along the glacier. Terminal moraines mark the furthest extent of glacial advance, while lateral moraines accumulate along the glacier's sides. In the Alps, the most distinct lateral and terminal moraines are those formed during the Little Ice Age (LIA), which represent the maximum extent of glaciers in the recent past. These moraines are particularly easy to identify in the field due to their sharp ridges and positioning, making them valuable markers for mapping past glacial extents. The deposition of sediments by meltwater channels in proglacial environments results in the formation of fluvial deposits, which are commonly associated with braided river systems due to their dynamic flow regime, high sediment supply and sorting of sediment fractions (Church and Ryder, 1972). The accumulation of meltwater behind a natural barrier at the glacier margin results in the formation of a proglacial lake. Alpine proglacial lakes often develop due to ice-damming, moraine-damming or in overdeepened bedrock basins shaped by glacial erosion (Buckel et al., 2018). The interaction between the meltwater channels and standing water bodies leads to the development of deltas, where sediment progradation occurs as particles settle from suspension (Bennett and Glasser, 2009). Changes in glacier dynamics, whether through advance or retreat, alter the meltwater and sediment supply, thereby influencing delta characteristics.

Meltwater channels may grow or dry out, leading to the migration of the delta along the ice margin.

Periglacial processes, occurring in cold, non-glacial environments, govern sediment redistribution and contribute to the evolution of alpine landscapes. A dominant characteristic of periglacial landscapes is the presence of permafrost. Permafrost defines any terrain, including soil or rock, along with any ice and organic material inclusions, that remains continuously frozen (at or below 0°C) for a minimum duration of two years consecutively (Muller, 1945). In cold mountain regions, permafrost is abundant in rock slopes at high elevations within different landforms such as bedrock, talus deposits and rock glaciers. Rock glaciers develop when rockfall material from surrounding slopes accumulates over an ice-rich core, insulating the buried ice from melting. The presence of the ice within the frozen ground enables rock glaciers to flow slowly downslope (Humlum, 2000). The insulating debris layer undergoes seasonal freeze-thaw cycles, which facilitate continuous deformation and advance of the rock glacier.

In addition to glacial and periglacial processes, gravitational processes contribute to the modification of alpine landscape. The combined effects of frost weathering and rockfall activity result in the development of talus cones and deposits through the progressive accumulation of rock debris at the base of steep slopes. Furthermore, rock fall activity is closely linked to debris-covered glaciers, as rockfall material can insulate glacier ice, influencing melt rates and glacier dynamics (Anderson et al., 2018).

06 METHODS

Mapping

In August 2024, fieldwork was conducted to map the Bachfallenferner glacier margin and forefield, with particular attention to supraglacial features. A high-resolution aerial survey was carried out using a MAVIC Mini 4 Uncrewed Aerial Vehicle (UAV), which provided detailed imagery of the study area, covering an area of approximately 2 km^2. Individual photographs have a resolution of 4032 × 2268 pixels, and were taken with a focal length of 6.72. A total of 4995 aerial photographs were captured and subsequently processed using Agisoft Metashape Professional 2.1.3. The processing followed a standard batch workflow, which involved aligning the images, generating a dense point cloud, creating a 3D model with texture, constructing a mesh, calculating a digital elevation model, and producing an orthomosaic. The generated 3D model offered both angled and overhead views of specific features, while the orthomosaic and digital elevation model (DEM) served as the basis for mapping *(Fig. 4)*. Mapping was then performed in QGIS, with all spatial data georeferenced according to the MGI/Austria GK West projection. To investigate the long-term evolution of the Bachfallenferner and its forefield, historical satellite imagery, provided by tiris (Amt der Tiroler Landesregierung, Abteilung Geoinformation, Geodaten und tiris, 2024) was analysed. The selection of specific years was guided by image quality, with 1973, 1997, 2009, 2015, 2018 and 2023 chosen as representative snapshots. These images offer valuable insights into changes in glacier extent, surface characteristics, and geomorphological transformations over time, complementing the field observations and high-resolution aerial data. Additionally, they enabled an expansion of the study area toward the north, east, and particularly west, offering a detailed view of features further downvalley. As a result, the total study area was extended to 7.5 km². For these expanded areas the 2023 satellite images served as the most recent basis for mapping. Preexisting GIS shapefiles of the glacier extent for 1997 and 2015 (Austrian Glacier Inventory, (Fischer et al., 2015; Buckel et al., 2018)) were used for mapping.

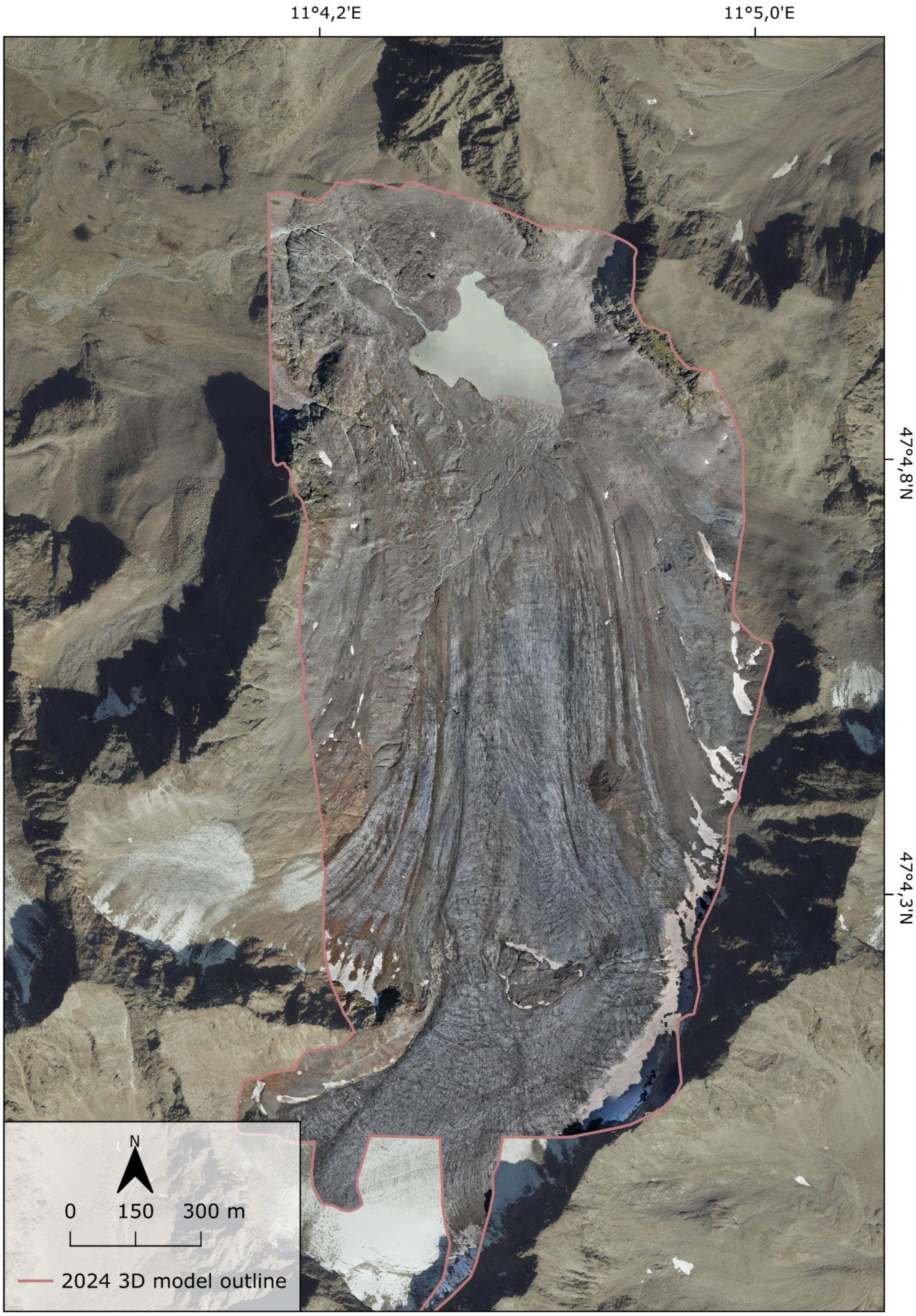

Figure 4: Orthophoto, 2023 (Amt der Tiroler Landesregierung, Abteilung Geoinformation, Geodaten und tiris, 2024, downloaded November 12, 2024 from data.tirol.gv.at) and orthomosaic of 3D model, 2024, of the study site

Clast Analysis

In addition to the mapping efforts, a clast analysis was conducted to determine the origin of deposits found in debris stripes on both sides of the glacier, as well as at the ice margin. Field sampling was carried out at three distinct locations. The first sampling site (CA1) was a debris stripe on the western side of the glacier, approximately 20 meters from the ice margin (47°04'34.4"N, 11°04'27.2"E). The second site (CA2) was at the northern end of the glacier in an ice-free area (47°04'43.9"N, 11°04'33.6"E). The third site (CA3) was near the southeastern side of the glacier, which is characterized by debris-covered ice (47°04'47.0"N, 11°04'39.5"E). At each sampling location, 30 randomly selected clasts were analysed based on seven parameters. The length of each clast was measured along the orthogonal a-, b-, and c-axis, representing the longest, second longest, and shortest dimensions, respectively, with measurements recorded in millimetres. Clast roughness was also assessed, with classifications ranging from angular (A) and subangular (SA) to subrounded (SR) and rounded (R). Additionally, the presence of faceted faces, striations, or scratches on the clasts was documented. The lithology of each clast was also described as part of the analysis, providing further insight into the composition and origin of the deposits.

The further processing of the clast analysis data was carried out using the Tri-Plot method according to Graham and Midgley (2000). For the Tri-Plot method, based on Sneed and Folk (1958), triangular diagrams are used to analyse sediment particle shape. By plotting the ratios of the three orthogonal axes of clasts they can be classified into blocks, slabs, and rods, allowing comparisons between various depositional environments *(Fig. 5)*. In glacial settings, this method is valuable for distinguishing between sediments actively transported by traction at the glacier bed (subglacial) and those passively carried withing the ice (englacial) or in its surface (supraglacial) (Benn and Ballantyne, 1997). However, even with the same catchment, varying lithologies can respond in different ways to erosional, depositional and transportational processes (Lukas et al., 2013), therefore, the interpreter must be cognisant of the influence of parent rock on clast shape (e.g. pelite tending to produce slab-shape clasts). The significant parameter within this method is the C40 index, which represents the ration of the shortest to longest particle axis (c:a). It has been shown to effectively separate sediments transported subglacially, where clast undergo greater abrasion and shape alteration, from those carried englacially or supraglacially, which tend to retain their original angularity.

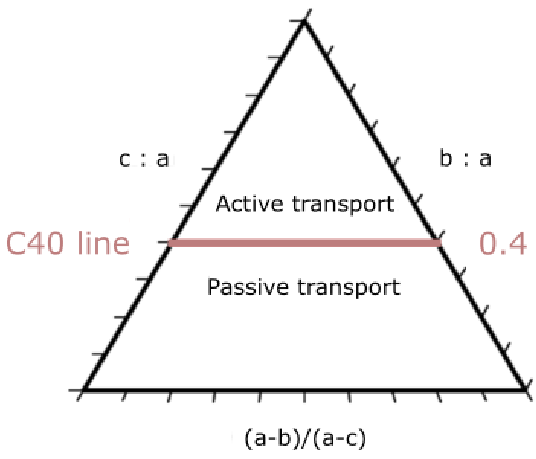

Figure 5: Tri-plot method: Triangular diagram is used to analyse sediment particle shape and assess sediment transport history (Graham and Midgley, 2000)

07 RESULTS

Satellite Image Analysis

The primary objective of this thesis was to create a detailed map of the area surrounding the Bachfallenferner, capturing its state from a 2024 perspective as well as from the recent past (1997, 2009, 2015, 2018). This analysis revealed significant geomorphological and sedimentological changes, all closely linked to the retreat of the glacier.

A comparison between the satellite image of 1997 and the 2024 orthomosaic indicates that the glacier has retreated by 450 m over this period. In 1997, a small lake began to form along the ice margin. The proglacial lake was bordered by bedrock and talus deposits. Close to the lake shore, patches of till are visible in the 1997 satellite image. Earlier satellite imagery shows that these areas were still covered by the glacier in 1973, suggesting that the exposed till was of subglacial origin. At the southwestern end of the lake a small delta has formed. The necessary meltwater and sediment supply likely originated from subglacial or englacial channels, as the only visible supraglacial meltwater channels discharge into the northern part of the lake. Much of the glacier near its terminus is covered with debris, which is especially extensive on the eastern side, extending further up the glacier, where a debris cone has developed in the mid-eastern section *(Fig. 6)*.

By 2009, the proglacial lake had expanded significantly. The southeastern shore remained connected to the glacier margin, while in the southwest, the delta grew, occupying areas that were formerly ice-covered. As the delta increased in size, avulsion formed new proglacial meltwater channels which fed the active lobe, whereas older channels were abandoned. The debris-covered part of the glacier was restricted to the eastern side of the glacier *(Fig. 6)*.

The 2015 satellite image revealed the continued retreat of the Bachfallenferner and the further growth of the proglacial lake, leaving only a narrow connection to the glacier in the lake's southeastern corner. As the ice retreated the delta grew and shifted eastward, dominating the newly exposed area. Meltwater channels in the former western delta dried out, with all active channels now discharging into the southern and eastern ends of the lake. The debris-covered ice on the eastern part of the glacier extended even farther up than in previous years, while new debris stripes formed near the terminus on the western side of the glacier. Both 2009 and 2015 satellite images showed the debris cone extending in all directions *(Fig. 6)*.

In 2018, the lake expanded slightly in the southeastern corner, with only a slim ice contact along the southeastern shore. The delta, featuring an extensive network of braided rivers and fluvial deposits interspersed with patches of subglacial till, occupied the area between the glacier margin and the lake shore. Similar to the 2015 satellite image, only the eastern side of the delta was active, while the channels on the western side had dried out. Debris cover was limited to the eastern part of the glacier, where it merged with the growing debris cone in the mid-eastern region. In the upper part of the glacier, ongoing melting and subsequent ice thinning exposed bedrock in the glacier's centre *(Fig. 6)*.

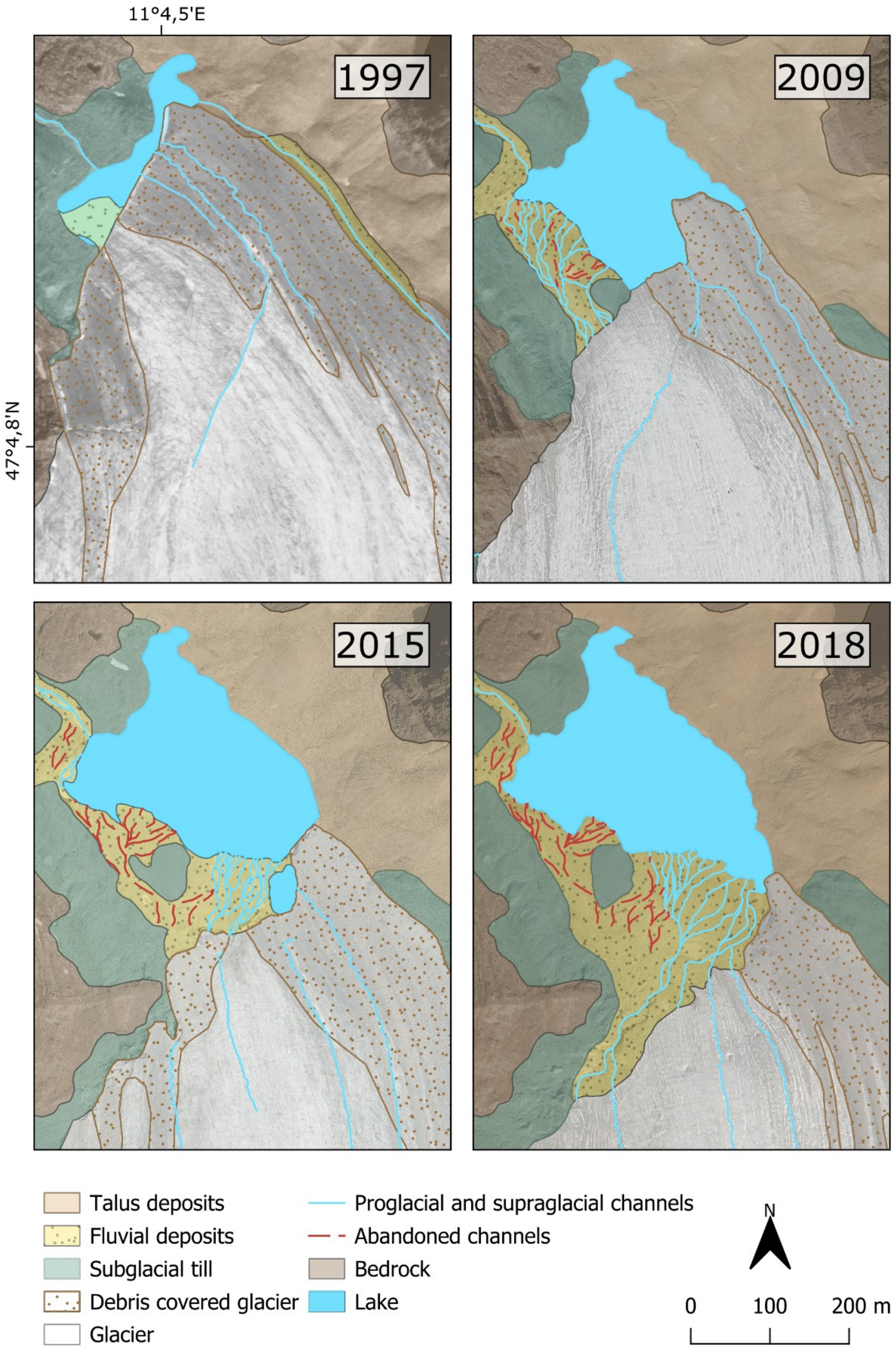

Figure 6: Geomorphological map illustrating changes in the ice margin, proglacial delta, and lake area across the years 1997, 2009, 2015, and 2018

Uncrewed Aerial Vehicle (UAV) Data Analysis

The 2024 orthomosaic generated from the 3D model permits high resolution mapping of the study area. This analysis is supplemented by incorporation of the 2023 satellite image, it was possible to expand more distant areas beyond the glacier, which were not captured by the drone flight.

The outline of the proglacial lake has remained mostly unchanged since the 2018 satellite image. Due to the accelerated retreat of the glacier, the ice and the lake are no longer connected. The delta, and its network of new meltwater channels, has expanded significantly *(Figure 7)*. In the western part of the delta, previously abandoned channels have been reactivated. Several flutes were mapped in the forefield (ranging 15 – 130 m away from the ice margin), surrounded by fluvial deposits and meltwater channels *(Figure 8)*. These flutes range from 5 – 35 m in length, 40 – 60 cm in height, and 70 – 100 cm in width. All the flutes are oriented perpendicular to the glacier front and consist of unsorted, loose, angular to sub-angular material, with a sand and silt matrix. The boundaries of the flutes are marked by large boulders (initiating boulder). Some flutes are cut off or split by meltwater channels. Supraglacial meltwater channels are present on the eastern, debris-covered section of the glacier, while proglacial meltwater channels from the upper western part of the glacier, which cut through bedrock, merge with supraglacial meltwater channels from the lower western section. A moulin located on the west side (47°04'31.3''N 11°04'28.9''E), approximately 14 m long and 7 m wide, has formed since 2020, with a large meltwater channel discharging into it *(Figure 9)*. On the east side of the glacier (47°04'25.4''N 11°04'45.8''E), nearly completely surrounded by debris-covered ice, the debris cone expanded significantly *(Figure 10)*. The cone itself is partially covered with debris, with clean ice visible all the way to its peak. The debris is angular and grey, with a brown eroded surface. The debris cone stands about 20 m high and stretches approximately 200 m in length. It is higher at the southern end, which appears to be the central part of the cone, it extends toward the southern end, where new material is deposited. Crevassing and deformation are evident southeast of the debris cone. The debris cover on the glacier consists of angular material and shows a discontinuous distribution. The individual blocks making up the cover can reach thicknesses of up to 10 - 30 cm. A lithological contrast is evident between the two sides of the glacier, with red-brown debris dominating the eastern flank and grey to dark material characterizing the debris stripes on the western side. The exposed bedrock in the centre of the glacier increased in size. At its western edge, only a narrow section, of thin ice, is connects the upper and lower part of the glacier.

As illustrated in the geomorphological map *(Figure 7)*, subglacial till on both sides of the glacier indicates areas previously overridden by ice. Gullies, along with active and inactive meltwater channels, cut through the till. In these till-dominated regions long, elongated debris stripes, orientated parallel to the flow direction, are present. The 1997 satellite image revealed debris stripes on the ice, near the current debris stripes, suggesting that these features have a supraglacial origin. As the glacier retreated, the debris stripes were deposited in proglacial areas. Their length, ranging from 150 – 220 m, far exceeds that of the mapped flutes, distinguishing them as separate structures.

Northwest of the lake, a prominent 400-m-long lateral moraine marks the LIA extent (Fischer et al., 2015). The former extent of the Bachfallenferner during the LIA can be traced further downvalley, where end moraines clearly define its maximum reach. Other lateral moraines were observed but could not be differentiated due to the absence of satellite imagery. Rock glaciers were clearly identified in the northwest, southwest and extensively in the southeast corner of the study area. Except for the rock glacier in the southwest, all exhibit signs of movement and are therefore classified as active. This aligns with observations from the literature (Krainer, 2015).

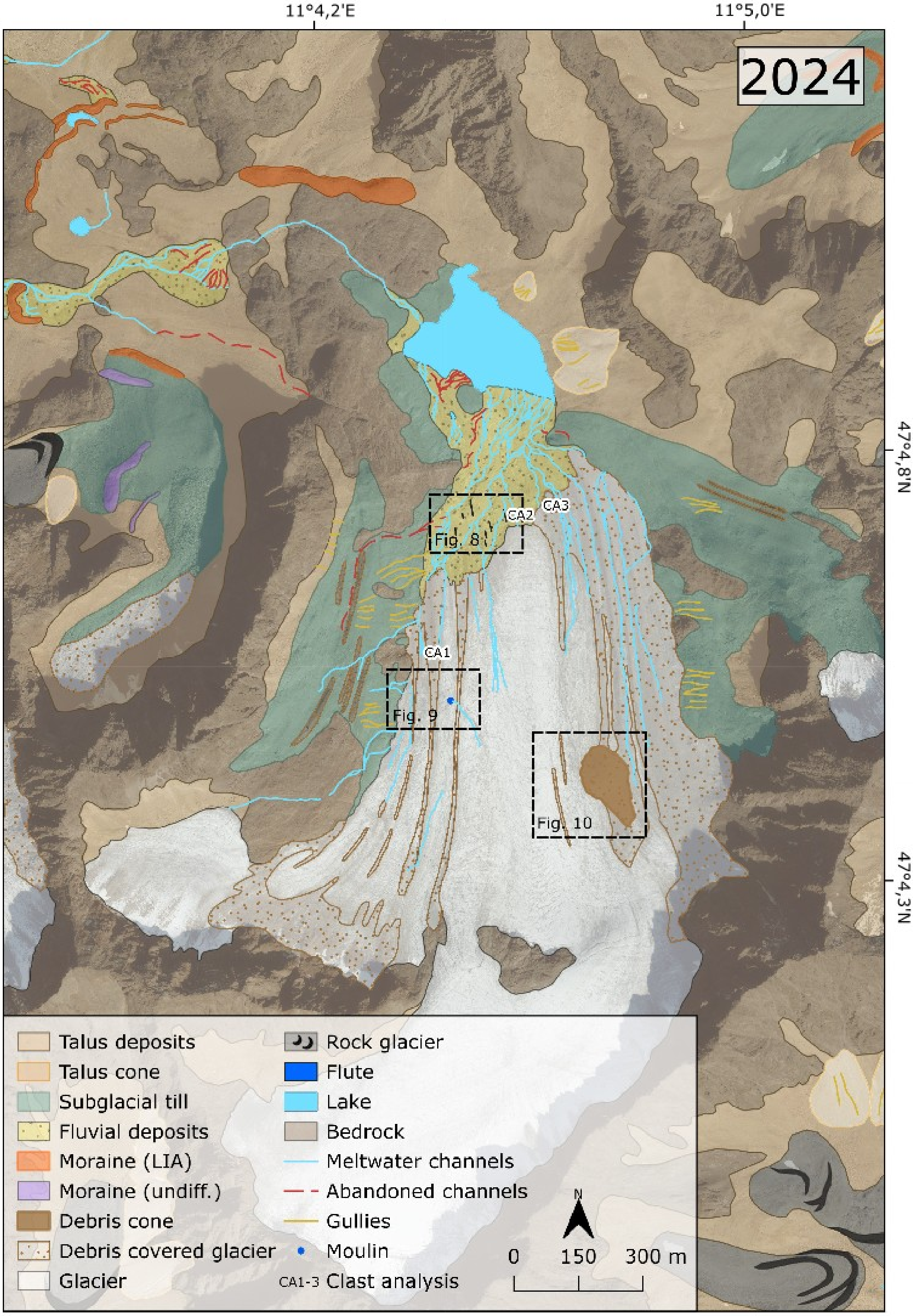

Figure 7: Geomorphological map of the Bachfallenferner region based on 2024 data

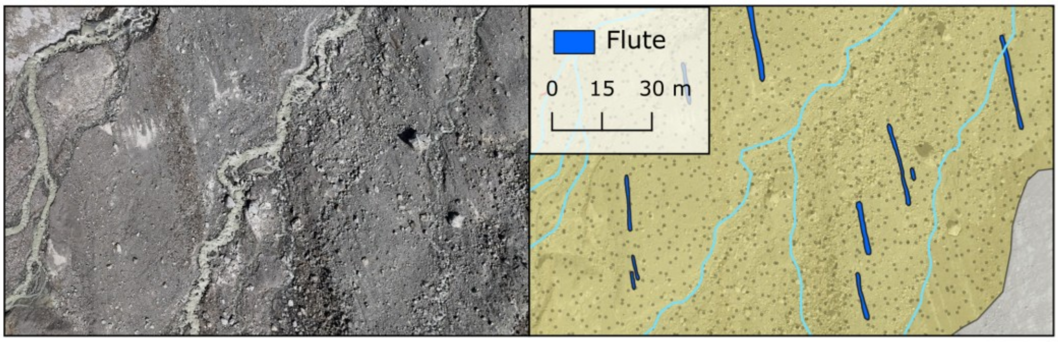

Figure 8: Flutes in the proglacial area, surrounded by meltwater channels

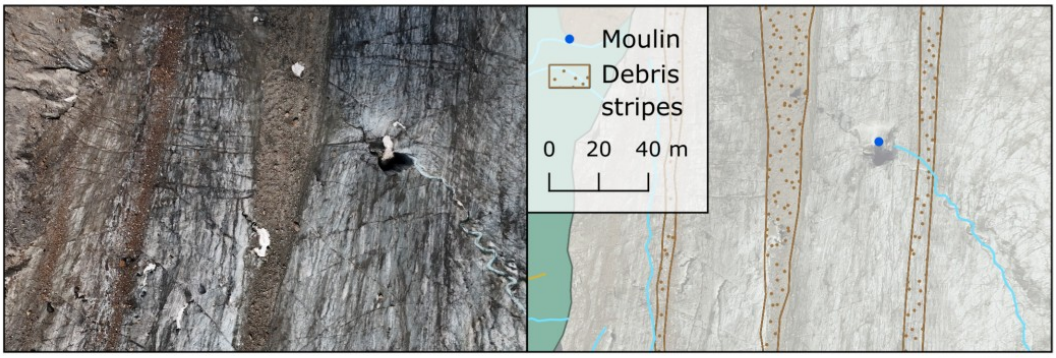

Figure 9: Moulin and debris stripes on the western side of the Bachfallenferner

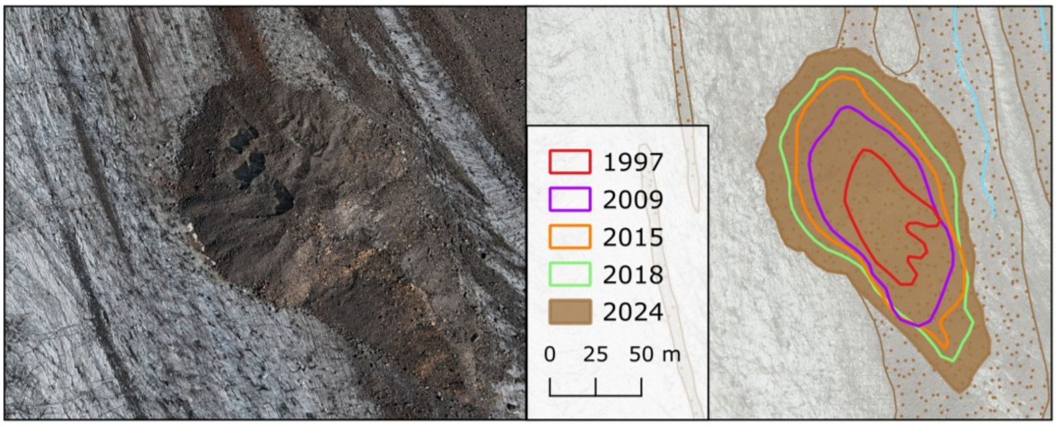

Figure 10: Aerial photograph of the debris cone (left) and evolution of the debris cone from 1997 to 2024 (right)

Sedimentary Deposits

Clast analysis provides insights into glacial transport dynamics by distinguishing between actively and passively transported debris based on roundness and shape ratios, particularly the c:a ratio (shortest axis to longest axis). Clasts that have been transported englacially or subglacially, classified as active transport, typically undergo significant abrasion, leading to more rounded or subrounded forms and higher c:a ratio. In contrast, passively transported clasts are carried supraglacially, often as rockfall debris deposited on top of the glacier. These clasts experience minimal abrasion, preserving their angular or subangular forms and resulting in lower c:a ratio (Lukas et al., 2013). According to the clast analysis presented here, the datasets CA1, CA2, and CA3 each display different transport regimes.

In CA1, 80% of the clasts exhibit a c:a ratio of less than 0.4, a clear indicator of passive transport processes (Benn and Ballantyne, 1997). The associated ternary plot *(Fig. 11-CA1)* presents a clustering of points underneath the C40 line, supporting this interpretation. The lithological composition of this dataset reveals a diverse lithological composition, with Mica-Schist making up the majority, followed by Quartz-Gneiss, Quartz-Clasts, Migmatite and Quartz-Schist. In contrast, CA2, shows a significantly different transport pattern, with over 80% of clast displaying a c:a ratio characteristic of active transport (Benn and Ballantyne, 1997). This is consistent with the ternary diagram *(Fig. 11-CA2)*, where clasts plot above the C40 line. The lithology distribution in this dataset mirrors CA1 to some extent, with Mica-Schist remaining the dominant component. However, Quartz-Gneiss is slightly more prominent in this dataset, while Quart-Clast, Quartz-Schist and Green-Schist are present but collectively account for less than one-fourth of the total. The higher degree of roundness aligns with subglacial or englacial movement, where mechanical abrasion smooths clast surfaces during transport. CA3 presents a transitional case. While the ternary plot *(Fig. 11-CA3)* shows a more mixed distribution, about two-thirds of the clasts still fall below the C40 line, suggesting a predominance of passive transport. Lithological diversity is lower than in the other datasets. Mica-Schist is overwhelmingly dominant, with only minor contributions from Quartz-Clast and Green-Schist.

While lithology can influence clast shape, since rocks with different strength and fracture behaviours respond differently to mechanical stress (Lukas et al., 2013), the consistent dominance of Mica-Schist across all three datasets reduces the impact of this factor. The ternary plots and shape analysis together suggest that CA1 and CA3 reflect more supraglacial deposition processes, while CA2 is shaped predominantly by subglacial or englacial transport.

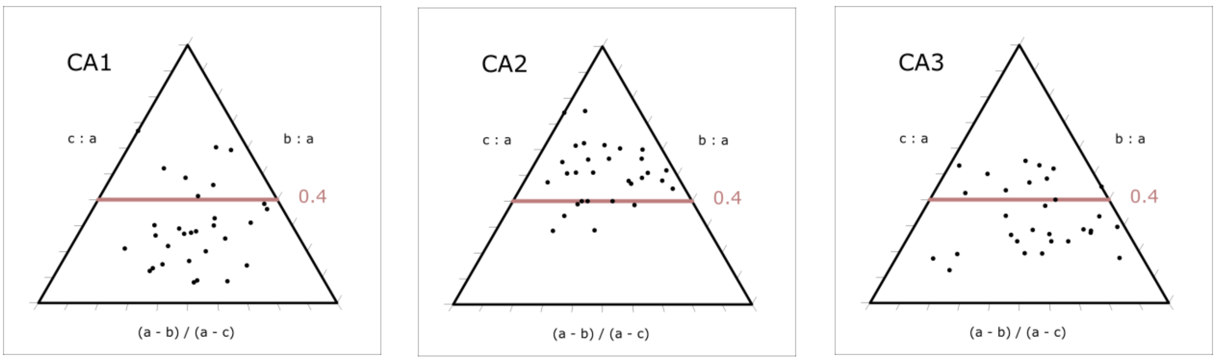

Figure 11: Trinary plots (after Graham and Midgley, 2000): CA1 – Clustering of points below the C40 line indicates supraglacial depositional processes; CA2 – Clustering of points above the C40 line suggests subglacial or englacial sediment transport; CA3 – Mixed distribution of points, with the majority below the C40 line, reflecting predominantly supraglacial transport

08 DISCUSSION

Based on interpretations from field observations, geomorphological mapping using both recent and historical data, and clast analysis, the following developments can be identified in the Bachfallenferner region.

Debris Cover

The amount of debris on the glacier, whether as debris stripes, debris cones or more extensive debris-covered zones, has increased significantly since 1997 *(Fig. 12).*

The origin of debris cover is primarily linked to material input from the surrounding topography. Clast analysis of supraglacial debris samples (C1 and C3) indicates that the dominant source is rockfall and backwasting from adjacent valley walls. In addition to direct surface input, debris deposited in the accumulation zone can become englacially incorporated. Once entrained, this material is transported via internal ice flow and meltwater channels, eventually re-emerging at the surface in the ablation zone as the glacier melts (Goodsell et al., 2005). Debris thickness generally increases downglacier, forming a longitudinal pattern characterized by a convex-up profile near the equilibrium line altitude (ELA) and a concave-up profile close to the glacier terminus (Anderson et al., 2018; Compagno et al., 2022). Glaciers exhibiting a negative mass balance, such as the Bachfallenferner (Lieb and Kellerer-Pirklbauer, 2024, 2025) typically show an expansion of debris-covered areas over time, especially as the ELA rises, causing more debris to melt out into the ablation zone (Stokes et al., 2007). All these factors explain the near-continuous debris cover close to the terminus of the Bachfallenferner and the relatively sparse debris in the upper part of the glacier, except beneath steep slopes directly influence by ongoing rockfall activity. Debris cover on the ice surface reduces the surface albedo, leading to increased net short-wave radiation (Østrem, 1959; Compagno et al., 2022). Thin debris layers (<2 cm) enhance ablation by absorbing more solar radiation (Compagno et al., 2022; Hénot et al., 2023), while thicker debris layers (> 4–10 cm) act as insulation, shielding underlying ice despite surface debris temperatures exceeding 15°C (Nicholson and Benn, 2006; Anderson et al., 2018). This insulation effect is crucial to the survival of features like debris cones and the persistence of lower glacier zones under thick debris.

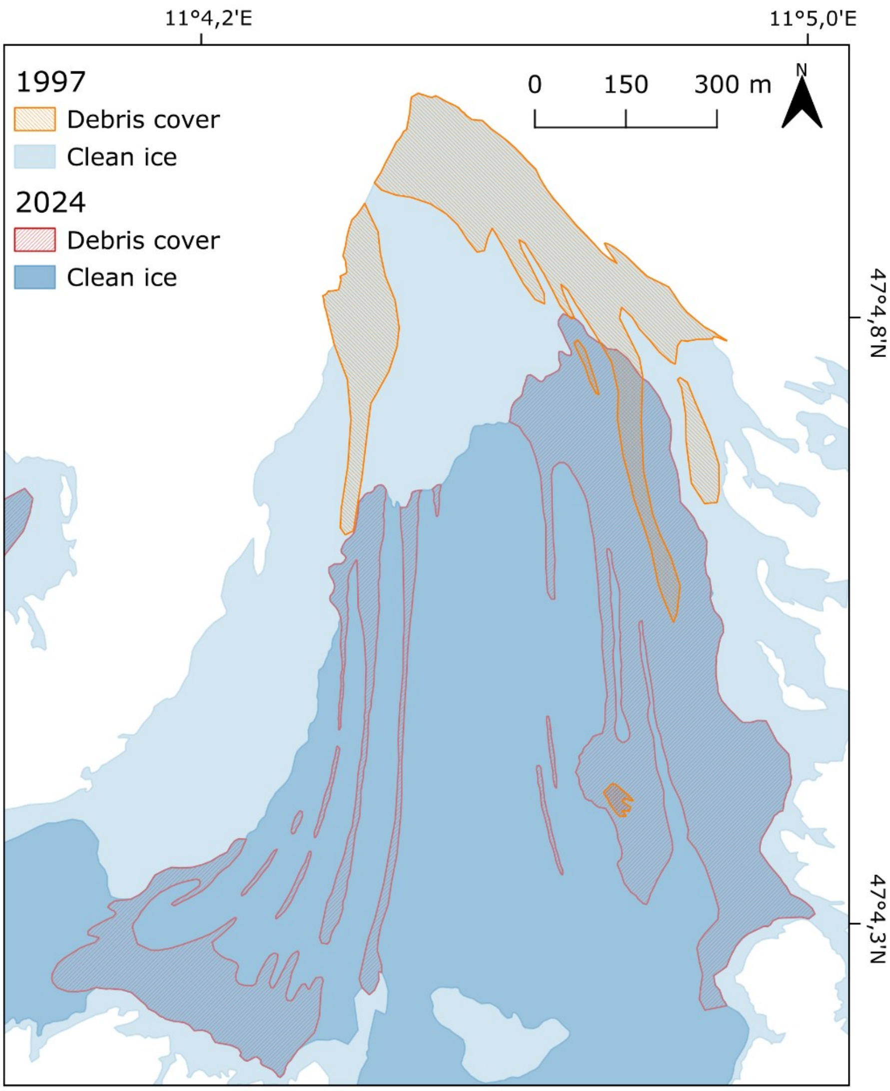

Figure 12: Comparison of debris cover extent from 1997 to 2024

Debris Cone

The presence of a prominent debris cone at Bachfallenferner highlights the complex interaction between debris supply, surface processes, and localized glacier dynamics. Satellite imagery and high-resolution orthophotos reveal no evidence of moulins or crevasses, typically associated with focused meltwater flow, which facilitates debris cone formation by concentrating debris in melt pits. The absence of such features suggests that an alternative mechanism is responsible for the cone development observed at the study site.

Mölg *et al.* (2020) introduced the concept of topographic inversion, whereby debris from steep backwasting valley walls is redistributed downslope, concentrating over small surface depressions. The insulating effect of this accumulated debris reduces ablation rates, allowing the underlying ice to persist while adjacent, debris-free areas continue to melt. Over time, this can invert the local surface topography, where a former depression becomes a topographic high, forming features such as dirt cones. Continuous glacier thinning emphasizes the prominence/local maximum of the cone.

Moreover, Hénot *et al.* (2023) highlight that debris cone growth is most efficient when the debris cover is thick enough to exceed the thermal conductivity threshold for insulation, typically around 4.9 cm for wet gravel. The cone on Bachfallenferner appears to maintain or exceed this threshold, possibly due to a continuous supply of coarse debris from upslope source. In contrast, the surrounding debris-covered ice, although also receiving material from nearly slopes, is characterized by a more patchy and discontinuous cover, which is insufficient to provide the same level of thermal protection.

In addition to direct insulation by surface debris, glacier ice can also be protected, resulting in locally reduced melt rates, by the influence of subglacial channels or englacial cavities. These drainage features can transport meltwater that is cooler than the surrounding ice, promoting local cooling through advective heat exchange (Werder et al., 2013). The Glacier Drainage System (GlaDS) model developed by Werder *et al.* (2013) simulates how distributed (characterized by high water pressure and low effective pressure) and channelized (low water pressure and high effective pressure) drainage systems affect basal friction. As the drainage transitions from a distributed to a channelized system, basal water pressure decreases, leading to an increase in basal friction and a deceleration of ice flow. Slower ice flow reduces strain heating and dynamic thinning, thereby decreasing the local energy available for surface ablation. In such zones, supraglacial debris may accumulate more readily, as reduced flow velocities limit the down-glacier transport of surface material.

In terms of debris cone genesis, three possible mechanisms *(Figure 13)* can be considered, namely (i) control via subglacial morphology, (ii) initiation via a major rockfall and (iii) a subglacial hydrology hypothesis. In the subglacial morphology hypothesis, a subglacial bedrock obstacle perturbed local ice flow, creating a preferential site for debris accumulation due to gravitational deposition of material from ongoing rockfall activity. The resulting debris cover reduced local ablation rates through thermal insulation, promoting the formation of the debris cone via differential surface lowering. However, there is no geomorphological or historical evidence indicating the presence of such an obstacle prior to the cone's initial appearance in the late 1990s, rendering this hypothesis unlikely. In a second model, the major rockfall hypothesis, debris initially concentrated on the ice surface via slope collapse. The insulating debris layer acted as an effective insulator, reducing surface melt and preserving the underlying ice.

Continued rockfall input, particularly on the stoss side of the cone, contributed to its asymmetric growth. Nevertheless, this theory lacks historical evidence on satellite image data of such a rockfall event. The lack of evidence for subsequent downglacier distribution of the material via surface meltwater flow or glacier ice deformation is also problematic. In a third model, englacial and subglacial hydrology plays an integral role. A localized subglacial drainage system delivered cold meltwater to the basal ice, reducing local surface ablation through hydrological decoupling (reduced basal sliding), local ice stiffening due to cooling, or uplift caused by increased basal water pressure. These processes could slow ice flow locally, favouring debris accumulation. Although the hypothesis that subglacial water flow alone could sufficiently reduce ablation from below, allowing enough time for supraglacial debris to accumulate to an insulating thickness, remains speculative, it is the most plausible of the three proposed models.

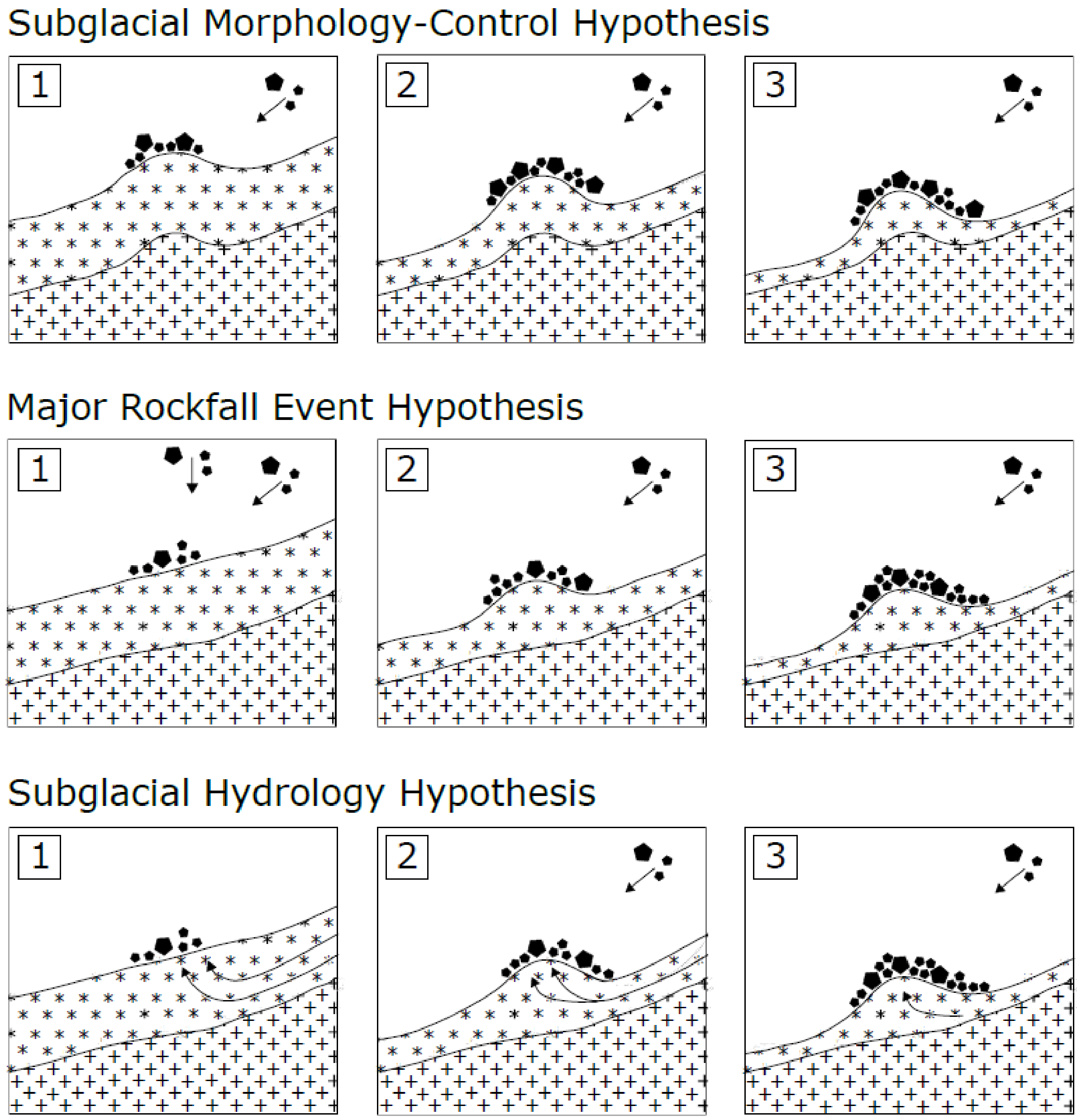

Figure 13: Proposed mechanisms for the formation of the debris cone on the eastern side of the Bachfallenferner

Delta Evolution

The proglacial delta has undergone significant transformation driven by changing meltwater dynamics, particularly due to increased glacier melt rates. This has led to a greater sediment supply, which directly reshapes the delta through expansion, infilling and the reworking of existing landforms Intensified meltwater flow has also reactivated older, abandoned channels, redirecting water across new parts of the delta. This process contributes to the erosion of previously stable features like flutes and disrupts the existing stratigraphy. These dynamic changes are associated with potential hazards such as delta front collapse. Nemec *et al.* (1988) explain that sustained and intense sediment input over time causes mechanical instability, due to processes such as overloading, underconsolidation and pore pressure buildup, which could trigger a glacier lake outburst

Proglacial Lake

Although the proglacial lake experienced a substantial expansion from 11.000 m^2 in 1997 to 53.000 m^2 in 2024, its susceptibility to glacial lake outburst floods (GLOFs) has decreased over the past decade. Emmer *et al.* (2015) describe the lake as a bedrock-dammed proglacial system in direct contact with the glacier ice. At that time (2015), due to the lake's contact with the ice, calving processes were still possible, creating a risk of displacement waves that could trigger a GLOF. From a present-day perspective, however, the glacier has retreated significantly, and the ice margin now lies 120 m form the lake shore, eliminating direct ice-lake contact. This retreat has eliminated the immediate GLOF risk associated with ice calving. Nonetheless, the lake remains a potential hazard, especially as it continuous to grow and is exposed to secondary mass movements, such as rockfalls resulting from permafrost degradation. Additionally, the rapidly increasing proglacial delta makes events such as delta front collapse more likely. These conditions can lead to sudden mass failures even in low-gradient delta systems. Recent events in Austria emphasize the continued relevance of such hazards. In 2016, a GLOF occurred at Goldbergkees (Glanz, 2018) in the Hohe Tauern region (Salzburg), followed by another at the Sulzenauferner (Piroton et al., 2024) in the Stubai Alps (Tirol) in 2018. Both events were linked to sudden spikes in meltwater production, triggered by extreme precipitation and anomalously high mean temperatures. These conditions accelerated glacier melt and increased outflow, highlighting the role of climatic extremes in amplifying glacial lake risks.

Future Development of the Bachfallenferner

The current state of the Bachfallenferner reflects trends observed in Austria's largest glaciers, such as the Pasterze in Carinthia, and serves as a small-scale analogue (Le Heron et al., 2022). Continued thinning is expected to lead to a complete detachment of the upper glacier from the lower tongue, particularly on the eastern side of the exposed bedrock, where the ice has already reached a critically low thickness. The resulting dead ice body, likely to be partially or entirely debris-covered, will no longer receive input from colder, dynamically flowing ice. Consequently, it becomes more vulnerable to atmospheric heating and enhanced surface ablation. The thickness, composition, and distribution of the debris cover will play a decisive role in determining the persistence and melt rate of this remnant ice mass.

09 CONCLUSIONS

- A new Quaternary geomorphological map is presented of the Bachfallenferner and its forefield. This is the first known mapping attempt of this area at a higher resolution

- Analysis of satellite imagery from 1997, 2009, 2015, 2018, and 2023, combined with UAV-based aerial photographs from 2024 and integrated with the mapping results, reveals significant changes over the 27-year-period. Key developments include: (i) enlargement of the proglacial lake and delta system, (ii) expansion of the debris-covered zone of the Bachfallenferner, (iii) formation of a substantial debris cone, and (iv) transition of a former icefall into an area of partially exposed bedrock.

- Three mechanisms are proposed to explain the origin of the prominent debris cone: (i) control by subglacial topography, (ii) initiation by a major rockfall event and (iii) processes related to subglacial hydrology.

- Mapping Alpine glaciers and their forefields is of critical importance, given the rapid and ongoing changes in their morphology. Differentiating between features such as debris stripes and flutes may prove challenging for future researchers due to their similar appearance. However, the presented geomorphological map effectively distinguishes between landforms of supraglacial and subglacial origin. In addition, it illustrates the substantial retreat of the Bachfallenferner over the past 27 years, evidence that points to a transition toward a dead ice body, a pattern already observed in numerous other Alpine glaciers.

ACKNOWLEDGMENTS

I would like to express my deepest gratitude to my supervisor, Univ.-Prof. Daniel Le Heron PhD whose guidance, encouragement, and expertise made this thesis possible. His support during the fieldwork and his ability to help me find the right direction at every stage of the thesis were invaluable.

My sincere thanks also go to my friends and colleagues from the Department of Geology for their companionship and motivation. I am especially grateful to Paulina Mejías-Osorio for her guidance, patience, and generosity in sharing her knowledge.

Finally, I wish to thank my family for their unwavering love and support throughout my years of study. Their constant support has been the foundation of my determination and success.

REFERENCES

Amt der Tiroler Landesregierung Abteilung Geoinformation, Geodaten und tiris, 2024. Land Tirol [WWW Document]. Land Tirol. URL data.tirol.gv.at (accessed 11.12.24).

Anderson, R.S., Anderson, L.S., Armstrong, W.H., Rossi, M.W., Crump, S.E., 2018. Glaciation of alpine valleys: The glacier – debris-covered glacier – rock glacier continuum. Geomorphology 127–142. https://doi.org/10.1016/j.geomorph.2018.03.015

Benn, D.I., Ballantyne, C.K., 1997. Reconstructing the transport history ofglaciogenic sediments – a new approach based on the co-varianceof clast form indexes. Sediment. Geol. 91, 215–227. https://doi.org/10.1016/0037-0738(94)90130-9

Benn, D.I., Evans, D.J.A., 2010. Glaciers and Glaciation. Hodder-Arnold, London, England.

Bennett, M.M., Glasser, N.F., 2009. Glacial Geology: Ice Sheets and Landforms, 2. ed. John Wiley & Sons, London.

Buckel, J., Otto, J., Prasicek, G., Keuschnig, M., 2018. Glacial lakes in Austria - Distribution and formation since the Little Ice Age. Glob. Planet. Change 164, 39–51. https://doi.org/10.1016/j.gloplacha.2018.03.003

Church, M., Ryder, J.M., 1972. A Consideration of Fluvial Processes Conditioned by Glaciation. Geol. Soc. Am. Bull. 83, 3059–3072.

Compagno, L., Huss, M., Miles, E.S., McCarthy, M.J., Zekollari, H., Dehecq, A., Pellicciotto, F., Farinotti, D., 2022. Modelling supraglacial debris-cover evolution from the single-glacier to the regional scale: an application to High Mountain Asia. The Cryosphere 16, 1697–1718. https://doi.org/10.5194/tc-16-1697-2022

Emmer, A., Merkl, S., Mergili, M., 2015. Spatiotemporal patterns of high-mountain lakes and related hazards in western Austria. Geomorphology 246, 602–616. https://doi.org/10.1016/j.geomorph.2015.06.032

Fischer, A., Kuhn, M., 2013. Ground-penetrating radar measurements of 64 Austrian glaciers between 1995 and 2010. Ann. Glaciol. 54. https://doi.org/10.3189/2013AoG64A108

Fischer, A., Seiser, B., Stocker Waldhuber, M., Mitterer, C., Abermann, J., 2015. Tracing glacier changes in Austria from the Little Ice Age to the present using a lidar-based high-resolution glacier inventory in Austria. The Cryosphere 9, 753–766. https://doi.org/10.5194/tc-9-753-2015

Glanz, M., 2018. Entwicklung und Zukunftsszenario des Gletschersees am Goldbergkees (Hohe Tauern). GEOGRAZ 62, 28–33.

Goodsell, R., Hambrey, M.J., Glasser, N.F., 2005. Debris transport in a temperate valley glacier: Haut Glacier d'Arolla, Valais, Switzerland. J. Glaciol. 51, 139–146. https://doi.org/10.3189/172756505781829647

Graham, D.J., Midgley, N.G., 2000. Graphical representation of particle shape using triangular diagrams: An Excel spreadsheet method. Earth Surf. Process. Landf. 25, 1473–1477. https://doi.org/10.1002/1096-9837(200012)25:13<1473::AID-ESP158>3.0.CO;2-C

Hammer, W., 1929. Erläuterung zur Geologischen Spezialkarte der Republik Österreich Blatt Ötztal. Geologische Bundesanstalt, Wien.

Hammer, W., 1925. Einige Ergebnisse der geologischenLandesaufnahme in den Westtiroler Zentralalpen. Geol. Rundsch. 16, 147–160.

Hammer, W., Ohnesorge, T., 1929. Geologische Spezialkarte, Blatt Ötzthal.

Hanzer, F., Förster, K., Nemec, J., Strasser, U., 2018. Projected cryospheric and hydrological impacts of 21st century climate change in the Ötztal Alps (Austria) simulated using a physically based approach. Hydrol. Earth Syst. Sci. 22, 1593–1614. https://doi.org/10.5194/hess-22-1593-2018

Helfricht, K., Huss, M., Fischer, A., Otto, J., 2019. Calibrated Ice Thickness Estimate for All Glaciers in Austria. Front. Earth Sci. 7. https://doi.org/10.3389/feart.2019.00068

Hénot, M., Langlois, V.J., Plihon, N., Taberlet, N., 2023. How dirt cones form on glaciers: field observation, laboratory experiments andmodeling. Phys. Rev. E 107, 034905. https://doi.org/10.1103/PhysRevE.107.034905

Hoinkes, G., 1973. Die Anatexis des Winnebachgranites (Ötztaler Alpen, Österreich) am Beispiel eines Aufschlusses. Tschermaks Min Petr Mitt 20, 225–239.

Hoinkes, G., Krainer, K., Tropper, P., 2021. Ötztaler Alpen, Stubaier Alpen und Texelgruppe, 3rd ed, Sammlung geologischer Führer. Gebrüder Borntraeger, Stuttgart, Germany.

Hoinkes, G., Purtscheller, F., Schantl, J., 1972. Zur Petrographie und Genese des Winnebachgranites (Ötztaler Alpen, Tirol). Tschermaks Min Petr Mitt 18, 292–311.

Humlum, O., 2000. The geomorphic significance of rock glaciers: estimates of rock glacier debris volumes and headwall recession rates in West Greenland. Geomorphology 35, 41–67. https://doi.org/10.1016/S0169-555X(00)00022-2

Ives, L.R.W., Iverson, N.R., 2019. Genesis of glacial flutes inferred from observations at Múlajökull, Iceland. Geology 47, 387–390. https://doi.org/doi.org/10.1130/G45714.1

Klötzli-Chowanetz, E., Klötzli, U., Koller, F., 1997. Lower Ordovician migmatisation in the Ötztal crystalline basement (Eastern Alps, Austria): Linking U-Pb and Pb-Pb dating with zircon morphology. Schweiz Miner. Petrogr Mitt 77, 315–324.

Krainer, K., 2015. Blockgletscher in den Ötztaler und Stubaier Alpen: Eine Übersicht. Publ. Alp. Forschungsstelle Obergurgl 4, 33–54.

Kumar, R., 2011. Glacier Pothole, in: Encyclopedia of Snow, Ice and Glaciers. Encyclopedia of Earth Sciences Series. Springer, Dordrecht.

Lambrecht, A., Kuhn, M., 2007. Glacier Changes in the Austrian Alps During the Last Three Decades, Derived from the New Austrian Glacier Inventory. Ann. Glaciol. 46, 177–184. https://doi.org/10.3189/172756407782871341

Lieb, G.K., Kellerer-Pirklbauer, A., 2025. Gletscherbericht 2023/24. Mitgliedermagazin Österr. Alpenvereins - Bergauf 1, 12–25.

Lieb, G.K., Kellerer-Pirklbauer, A., 2024. Gletscherbericht 2022/23. Mitgliedermagazin Österr. Alpenvereins - Bergauf 2, 11–21.

Lukas, S., Benn, D.I., Boston, C.M., Brook, M., Coray, S., Evans, D.J.A., Graf, A., Kellerer-Pirklbauer, A., Kirkbride, M.P., Krabbendam, M., Lovell, H., Machiedo, M., Mills, S.C., Nye, K., Reinardy, B.T.I., Ross, F.H., Signer, M., 2013. Clast shape analysis and clast transport paths in glacial environments: A critical review of methods and the role of lithology. Earth-Sci. Rev. 112, 96–116. https://doi.org/10.1016/j.earscirev.2013.02.005

Mölg, N., Ferguson, J., Bolch, T., Vieli, A., 2020. On the influence of debris cover on glacier morpholgy: How high-relief structrues evolve from smooth surfaces. Geomorphology. https://doi.org/10.1016/j.geomorph.2020.107092

Muller, S.W., 1945. Permafrost or Permanently Frozen Ground and Related Engineering Problems, 2nd ed. Army map service, U.S. Army.

Nemec, W., Steel, R.J., Gjelberg, J., Collinson, J.D., Prestholm, E., Oxnevad, I.E., 1988. Anatomy of collapsed and re-established delta front in Lower Cretaceous of eastern Spitsbergen: gravitational sliding and sedimentation processes. AAPG Bull. 72, 454–476.

Nicholson, L., Benn, D.I., 2006. Calculating ice melt beneath a debris layer using meteorological data. J. Glaciol. 52, 463–470. https://doi.org/10.3189/172756506781828584

Nicolussi, K., Le Roy, M., Schlüchter, C., Stoffel, M., Wacker, L., 2022. The glacier advance at the onset of the Little Ice Age in the Alps: New evidence from Mont Miné and Morteratsch glaciers. The Holocene 32, 624–638. https://doi.org/10.1177/0959683622108824

Østrem, G., 1959. Ice Melting under a Thin Layer of Moraine, and the Existence of Ice Cores in Moraine Ridges. Geogr. Ann. 41, 228–230. https://doi.org/10.1080/20014422.1959.11907953

Piroton, V., Emmer, A., Schlögel, R., Hřebřina, J., Pummer, E., Mergili, M., Havenith, H., 2024. Geomorphological processes and landforms in the AlpineSulzenau Valley (Tyrol, Austria): Glacier retreat, glacial lakeevolution and the 2017 glacial lake outburst flood. Earth Surf. Process. Landf. 49, 4823–4841. https://doi.org/10.1002/esp.5956

Reitner, J., 2022. The Imprint of Quaternary Processes on the Austrian Landscape, in: Landscapes and Landforms of Austria. Springer International Publishing, Cham, pp. 47–72.

Schindlmayr, A., 1999. Granitoids and Plutonic Evolution of the Ötztal-Stubai Massif – A Key for Understanding the Early Palaeozoic History of the Austroalpine Crystalline Basement in the Western Eastern Alps. Univ. Salzburg, Salzburg.

Sneed, E.D., Folk, R.L., 1958. Pebbles in the lower Colorado River, Texas, a study of particle morphogenesis. J. Geol. 66, 114–150.

Stadt Wien und Österreichische Länder bzw. Ämter der Landesregierung, 2021. Geoland Basemap Orthofoto [WWW Document]. basemap.at. URL https://maps.wien.gv.at/basemap/1.0.0/WMTSCapabilities.xml

Stokes, C.R., Popovnin, V., Aleynikov, A., Gurney, S.D., Shahgedanova, M., 2007. Recent glacier retreat in the Caucasus Mountains, Russia, and associated increase in supraglacial debris cover and supra-/proglacial lake development. Ann. Glaciol. 46, 195–203. https://doi.org/10.3189/172756407782871468

Swithinbank, C., 1950. The Origin of Dirt Cones on Glaciers. J. Glaciol. 1, 461–465. https://doi.org/10.3189/S0022143000012880

van Husen, D., 1997. LGM and late-glacial fluctuations in the Eastern Alps. Quat. Lnternational 38/39, 109–118. https://doi.org/10.1016/s1040-6182(96)00017-1

World Glacier Monitoring Service, 2024. Fluctuations of Glaciers Database. https://doi.org/10.5904/wgms-fog-2024-01